

Programming magnetic ordering for smart micromachines

by Yuan LIU

Thesis submitted in fulfilment of the requirements for
the degree of

Doctor of Philosophy

under the supervision of Prof. Dayong JIN, Dr. Gungun LIN,
Dr. Fan WANG

University of Technology Sydney
Faculty of Science

03/03/2021

Certificate of Original Authorship

I, Yuan LIU declare that this thesis is submitted in fulfilment of the requirements for the award of Doctor of Philosophy, in the School of Mathematical and Physical Sciences, Faculty of Science, at the University of Technology Sydney.

This thesis is wholly my own work unless otherwise reference or acknowledged. In addition, I certify that all information sources and literature used are indicated in the thesis.

This document has not been submitted for qualifications at any other academic institution.

This research is supported by an Australian Government Research Training Program.

Signature: Production Note:
Signature removed prior to publication.

Date: 03/03/2021

Acknowledgements

Completing a PhD thesis is one of life's biggest achievements. During the four-year study, I received much help from a lot of people. I would like to express my deep and sincere gratitude to these people.

First of most, to my principal supervisor, distinguished Prof. Dayong Jin, I am grateful for the opportunity to complete my research topic. He provided me with a first-class research platform and the funding that made it possible. He taught me how to face the challenges that experiments pose.

To my co-supervisor, Dr Gungun Lin, thank you for your patience and guidance in my projects. He led me into the new research field, this being magnetic soft matter. He guided me on how to search the research topic, develop the plan of attack, and discover the underlying science from an experiment perspective.

I would like to address a special thanks to Dr. Denys Makarov and Mr Ingolf Mönch for the help of magnetic sensor fabrication, Dr. Fan Wang for helping set up optical imaging system, Dr Yinghui Chen for the analysis chemistry aspects, Dr Hongxu Lv and Miss Guan Huang for their help of cell culture. I would like to mention all my colleagues at IBMD who gave me advice and help for my projects. I found I was so happy to work with them and I will remember them forever.

I would like to thank my family members for their support and understanding. In particular, I thank my fiance Siyu Huang, for her understanding, sympathy and incalculable contribution.

Finally, I would like to acknowledge the ARC Research HUB and the China Scholarship Council Scholarship for providing me with the scholarship.

Format of Thesis

This is a conventional thesis consisting of 6 chapters. Chapter 1 is an introduction chapter with a comprehensive literature review. The background, motivation, advances made in magnetic micromachines, challenges, and bioinspired magnetoreception are discussed in detail.

Chapter 2 discusses representative approaches to fabricate ordered magnetic structures.

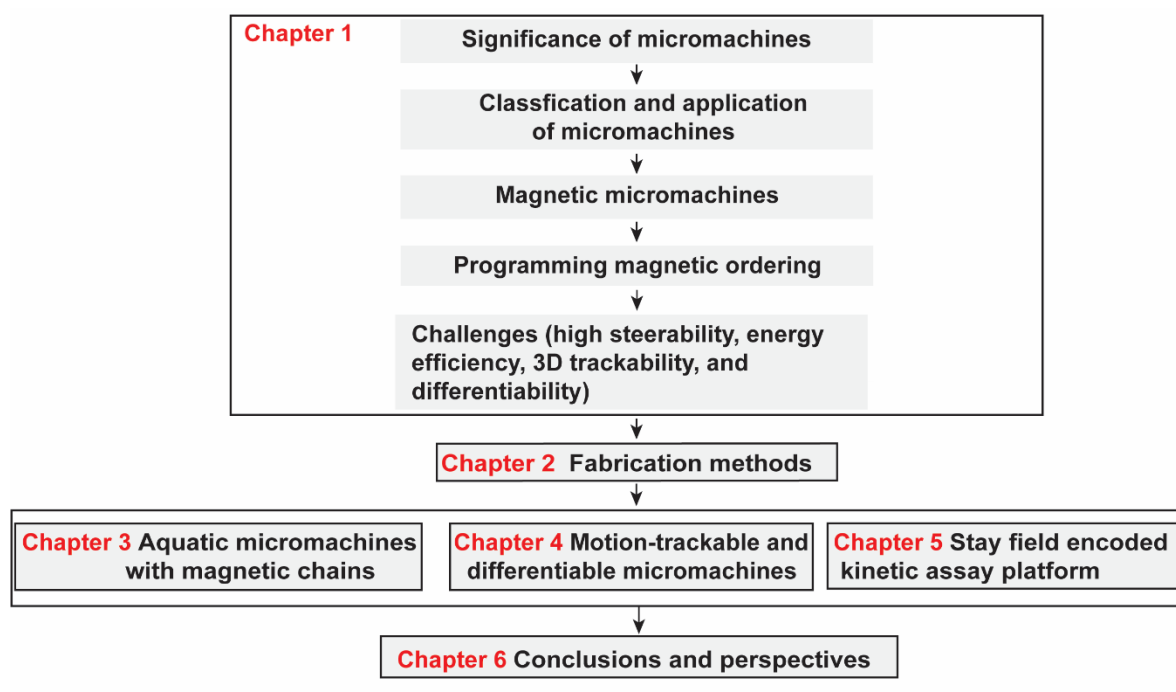
Chapter 3-5 summarise previous investigations of magnetic micromachines with ordered structures.

Chapter 3 examines aquatic micromachines with new functionalities induced by ordering magnetic nanoparticles in polymers.

Chapter 4 introduces 3D motion-trackable and differentiable micromachines based on the compartmentalization assembly of micrometer-scale magnetic building blocks.

Chapter 5 further reports a novel stay-field encoded kinetic assay platform based on the compartmentalization assembly of magnetic building blocks.

Chapter 6 summarizes the main research outcomes of the PhD dissertation and possible future research directions that may arise based on the advances made .



List of Publications

Articles

1. Yuan Liu[†], Gungun Lin^{†*}, Yinghui Chen, Ingolf Mönch, Denys Makarov, Bradley J. Walsh, Dayong Jin* "Coding and decoding stray magnetic fields for multiplexing kinetic bioassay platform." *Lab Chip*, 2020,20, 4561-4571. (Cover page of journal: *Lab Chip*, 2020,20, 4506-4506.)
2. Gungun Lin[†], Yuan Liu[†], Guan Huang, Dr. Yinghui Chen, Dr. Denys Makarov, Jun Lin, Prof Zewei Quan, Dayong Jin, "3D Rotation-trackable and Differentiable Micromachines with Bioinspired Magnetoreception for Complex and Dynamic Bioanalysis", *Advanced Intelligent Systems* (2020): 2000205. (Cover page of journal: *Advanced Intelligent Systems* (2021): 202170020)
3. Yuan Liu[†], Gungun Lin[†], Dayong Jin "“Universal Stratified-Disk Architecture for Micro-robotic Functionalization”, Submitted.
4. Fang, Guocheng, Hongxu Lu, Hamidreza Aboulkheyr Es, Dejiang Wang, Yuan Liu, Majid Ebrahimi Warkiani, Gungun Lin, and Dayong Jin. "Unidirectional intercellular communication on a microfluidic chip." *Biosensors and Bioelectronics* (2020): 112833.

Patents

Dayong Jin, Gungun Lin, Yuan Liu, "Anisotropic magnetic particles", Australia patent, Lodged. AU2020/903646

Table of Symbol

τ_N	Néel relaxation time
k_B	Boltzmann constant
T	temperature of surrounding environment
K	density of magnetic anisotropy energy
τ_0	attempt time
Re	Reynolds number
ρ_l, ρ	density of the liquid and machine body
μ_l	viscosity of the liquid
\vec{H}	external magnetic field
\vec{B}	magnetic flux density
\vec{M}	magnetization
\vec{M}_r	remanent magnetization
H_{ci}	intrinsic coercivity
\vec{m}_1, \vec{m}_2	magnetic moments of the cores
$\vec{m}_{p1}, \vec{m}_{p2}$	permanent moments of the cores
$\vec{m}_{i1}, \vec{m}_{i2}$	induced magnetic moments of the cores
\hat{r}	unit vector parallel to the line joining the centers of the two magnetic cores/dipoles
μ_0	vacuum permeability
μ_r	relative permeability
r_1, r_2	radius of the micro-scale cores
L	distance between two interacting magnetic cores/dipoles
r_0	radius of the mesoscopic magnetic cores

L_0	spacing between the mesoscopic magnetic cores
χ	magnetic susceptibility
E, E_i, E_p	magnetic energy, energy components of induced moment and permanent moment, respectively
$\varphi_f, \varphi_i, \varphi_{ma}$	magnetic energy, energy components of induced moment and permanent moment
$\vec{\omega}_{ma}$	rotation frequency of magnetic micromachines
\vec{m}_n	magnetic moment of the n^{th} nanoparticle
N	total number of nanoparticles
ε	shape factor
η	viscosity of the liquid
θ	angle between the magnetic field and uniaxial orientation
l	scale factor of the machine body
F_s	sliding friction force
μ_s	coefficient of kinetic friction
F_n	normal force
C_{rr}	coefficient of rolling friction
U, U_1	interparticle interaction energy
H_e	induced magnetic field from
F_c	centrifugal force
R_{rv}	revolution radius
ω_m, ω_{rv}	angular rotation frequency of the magnetic field and revolution frequency of micromachines
α_{slip}	slipping probability
$F_{\text{surface tension}}$	lifting force exerted on aquabots from the surface tension for floating
F_{gravity}	gravitational force

γ	surface tension coefficient of the water
h_d	height of disk-shaped micromachines
r_d	radius of disk-shaped micromachines
g	gravity
F_i	interfacial force
F_s	shear force
d	diameter of a droplet
Q_1, Q_2, Q_3	Flow rates of inner, middle and outer phase
Q_c, Q_d	flow rate of the continuous phase and disperse phase
l_d	droplet neck width
D	diameter of a collection capillary
ν	droplet generation frequency
D_1, D_2, D_3	diameter of inner, middle and outer capillaries
ν_1, ν_2	droplet generation frequencies of two emulsification steps
N	ratio of droplet generation frequencies (ν_1 and ν_2)
α, β, φ	rotation angle along the x-, y- and z-axis.
$R_x(\alpha), R_y(\beta),$ $R_z(\varphi)$	rotation matrices that rotate a vector around the x, y, and z-axes
B_s	total effective field that can be detected by a GMR sensor stripe
d_1, d_2, d_3	inter-peak/valley distance of a voltage signal profile of a microparticle.
S_i	space ratio of inter-peak/valley distance
W_{GMR}, L_{GMR}	width and length of the GMR sensor
V_m	magnetic scalar potential

Abbreviations

MNPs	magnetic nanoparticles
SPION	superparamagnetic iron oxide nanoparticles
PAH	poly(allylamine hydrochloride)
PSS	poly-(sodium 4-styrenesulfonate)
PEG-DA	poly(ethylene glycol) diacrylate
DVB	oilily divinylbenzene
OA	oleic acid
dMR	disk-shaped micromachines
sMR	stripe-shaped micromachines
DCM	dual-compartment micromachines
MMCs	mesoscopic magnetic cores
MTDM	3D rotation-trackable and differentiable micromachines
NdFeB	neodymium–iron–boron

Contents

Acknowledgements.....	i
Format of Thesis	iii
List of Publications	v
Table of Symbol	vi
Abbreviations	ix
Contents	x
List of Figures	xiii
List of Tables.....	xvii
Abstract	xviii
Chapter 1. Introduction.....	1
1.1. Smart micromachines.....	1
1.1.1. Definition of “smart micromachines”	1
1.1.2. Locomotion of micromachines	2
1.1.3. Typical propulsive mechanisms	4
1.2. Magnetic micromachines	15
1.2.1. Materials.....	15
1.2.2. Biocompatibility.....	23
1.2.3. Control and tracking system	25
1.3. Ordered magnetic structures	26
1.3.1. Magnetic anisotropy.....	26
1.3.2. Bio-magnetoreception with directionality	27
1.3.3. Ordered magnetic structures with dipolar magnetic coupling	28
1.3.4. Micromachines with magnetic orders	30
1.4. Challenges	37
1.5. Thesis aims and outline.....	39
Chapter 2. Fabrication methods.....	41
2.1. Photolithography	41
2.1.1. Photomask by laser writing.....	42
2.1.2. Materials.....	43
2.1.3. Fabrication of patterned magnetic micromachines	44
2.2. Microfluidics emulsification	44
2.2.1. Capillary devices based on the 3D printed mould	45
2.2.2. Surface treatment of glass capillaries.....	47
Chapter 3. “Euler’s Disk”-inspired Aquabots with Multimodal Locomotion and Dynamic Maneuverability.....	49
3.1. Background	49
3.1.1. Hierarchical motions	50
3.1.2. Large-area locomotion	52

3.2.	Euler's disk inspired locomotion	55
3.3.	Fabrication and characterisation of aquabots	56
3.3.1.	Design	56
3.3.2.	Prototype	57
3.4.	Results and discussions	58
3.4.1.	Mechanism of the multimodal underwater locomotion	58
3.4.2.	Environmental adaptability of aquabots.	69
3.5.	Conclusion and perspective.....	80
Chapter 4.	3D Rotation-trackable and Differentiable Micromachines with Bioinspired Magnetoreception for Complex and Dynamic Bioanalysis	82
4.1.	Background	83
4.2.	3D rotation-trackable and differentiable micromachines	84
4.2.1.	Bioinspired magnetoreception	84
4.2.2.	Elaborately engineered magnetic anisotropy	87
4.3.	Design and construction of micromachines via elaborately engineered magnetic anisotropy	88
4.3.1.	Multiphase microfluidic flow-mediated synthesis	88
4.3.2.	Construction of multi-compartment magnetic micromachine structures.	95
4.4.	Results and discussions	97
4.4.1.	Exploring synchronous-asynchronous rotation transition by structural variance	97
4.4.2.	Multi-axial positioning and dynamic evaluation of 3D multicellular constructs	107
4.4.3.	Parallelised analysis of distinctive biomolecular analytes	114
4.5.	Conclusions	117
Chapter 5.	Coding and Decoding Stray Magnetic Fields for Multiplexing Kinetic Bioassay Platform	119
5.1.	Background	120
5.2.	Discrete Magnetic codes with built-in magneto-capabilities Magnetic code library 121	
5.2.1.	Stray magnetic field fingerprints.....	121
5.2.2.	Kinetic assay platforms	123
5.3.	Synthesis of hierarchically-assembled core-shell magnetic microstructures	125
5.4.	Results and discussions	128
5.4.1.	Magnetic decoding with a GMR-based magnetic chip	128
5.4.2.	Exploring raster scanning mode.....	133
5.4.3.	Microfluidic flow cytometry	136
5.4.4.	Multiplexed DNAs assay based on the magnetic coding-decoding platform 139	
5.5.	Conclusions	143

Chapter 6. Conclusions and outlook	145
6.1. Conclusions	145
6.2. Outlook.....	147
6.2.1. Magnetic controlled system with micro-scale resolution	147
6.2.2. Motion tracking and control in clinically-relevant settings	148
6.2.3. Super-fast magnetic decoding system.....	149
6.2.4. Programming and Dynamic assembly of magnetic micromachines	149
References	151

List of Figures

Figure 1-1 Schematic of locomotion environment and physical restraints exerted on micromachines	2
Figure 1-2 Chemically powered microjets	6
Figure 1-3 Acoustically propelled motor.	7
Figure 1-4 Light-driven micro-rockets.....	8
Figure 1-5 Biologically propelled microrobots.....	10
Figure 1-6 Magnetically actuated microrobots	11
Figure 1-7 Mesoscopic structures of magnetic micromachines	14
Figure 1-8 Photolithography	22
Figure 1-9 Microfluidic emulsions.....	23
Figure 1-10 Ordered magnetic structures.....	29
Figure 1-11 Shape change of magnetic micromachines with multiple magnetic axes under the magnetic field.....	30
Figure 1-12 Magnetic actuation of ordered magnetic structures	32
Figure 1-13 Fabrication methods of small-scale machine with heterogeneous magnetic anisotropy	33
Figure 1-14 Controlled locomotion modes with a varying magnetic field	35
Figure 1-15 Flagelled soft machines with controlled morphologies.....	36
Figure 2-1 Schematic of photomask manufacturing process	42
Figure 2-2 Patterned microstructures fabricated by photolithography	43
Figure 2-3 Optimized exposure time for varying magnetic contents.....	44
Figure 2-4 Glass capillary device assembled by the 3D-printed T-junctions.....	45
Figure 2-5 Physics map of capillary device assembled by the 3-printed T-junctions..	46
Figure 2-6 Schematic of the layer-by-layer surface treatment.....	47
Figure 3-1 Motion of celestial bodies	53
Figure 3-2 Large-area circular motions of artificial satellites.....	54
Figure 3-3 Hierarchical gyration of a ‘Euler’s disk’.	56
Figure 3-4 “Euler’s disk”-inspired “aquabots”.	56
Figure 3-5 Schematic illustration of the micro-fabrication process of magnetic micromachines	57
Figure 3-6 Micro-structures of micromachines fabricated directional magnetic fields	58
Figure 3-7 3D cyclic rotating magnetic field	58
Figure 3-8 Locomotion profile of magnetic micromachines.	60
Figure 3-9 Revolution of a disk-shaped micromachines without (left, dMR-1) and with (right, dMR-2) induced magnetic ordering	62
Figure 3-10 Schematic illustration showing the control of micromachines with a cyclic rotating magnetic field using a permanent magnet	62
Figure 3-11 Anisotropy-mediated stance control.	64

Figure 3-12 Multimodal pre-selectable locomotion of aquabots using magnetic anisotropy and morphological design	65
Figure 3-13 Brachiation of ellipsoidal micromachines with long-range magnetic ordering	66
Figure 3-14 Frequency response of multiple micromachines	67
Figure 3-15 Scatter plot distribution of motilities <i>versus</i> body mass of micromachines and other artificial microscale machines in relation to mammals and organisms.	68
Figure 3-16 Ascending a barrier	69
Figure 3-17 Schematic illustration of micromachines climbing a barrier	70
Figure 3-18 Complex barriers for underwater locomotion	70
Figure 3-19 ‘Smart’ locomotion with micromachines of varied lengths	71
Figure 3-20 Schematic of locomotion in 1D confined space	72
Figure 3-21 Locomotion of micromachines in a static condition, including rotation and revolution via frequency	72
Figure 3-22 Rotation of micromachines at 400 rpm under changing flow rates	73
Figure 3-23 Revolution of micromachines at 800 rpm under changing flow rates	74
Figure 3-24 Systematic study of the locomotion in the capillary	74
Figure 3-25 Sketch map of aquatic locomotion	75
Figure 3-26 Locomotion profile of aquabots	76
Figure 3-27 Collective motion of multiple micromachines at different rotation speeds of the magnetic field	77
Figure 3-28 Demonstration of the adaptability of micromachines to complex environments relevant to the hierarchical morphologies of the inner of an artificial gastrointestinal model featuring fluid-filled cavities and wrinkles	79
Figure 4-1 Bio-Magnetoreception	86
Figure 4-2 Conceptual illustration of the approach to distributing active mesoscopic magnetic cores (MMCs) in a polymer matrix to design MTDM	86
Figure 4-3 Bio-inspired smart micromachines with motion-decodable magnetoreception	87
Figure 4-4 Differentiable rotation states.	88
Figure 4-5 Analysis of flow-rate mediated emulsion formation	90
Figure 4-6 Influence of outer flow rate on emulsion generation.	91
Figure 4-7 Representative regimes of fabricating micromachines of different levels of magnetic order defined by dashed lines.	92
Figure 4-8 Flow-rate mediated fabrication of distinct highly-ordered structures):	94
Figure 4-9 Fabrication process of micromachines	96
Figure 4-10 Microscopy images of magnetic microstructures	97
Figure 4-11 Schematic illustration of spinning a dual-core micromachine	98
Figure 4-12 Time-dependent rotation angle	98
Figure 4-13 Critical rotation frequency of single-compartment micromachines	100

Figure 4-14 Dependence of the required magnetic field strength to rotating different micromachine structures to the same critical frequency of 10 Hz.	101
Figure 4-15 Plot of the critical rotation frequency (f_{critical}) against the geometric factor, $r_1 r_2 / (r_1 + r_2)$ of dual-compartment micromachines.	105
Figure 4-16 Dependence of the rotational properties of the hydrogel composite on fluid conditions.	106
Figure 4-17 Critical rotation frequency under modulated temperature and glycerol concentration.	107
Figure 4-18 3D rotational navigation.	108
Figure 4-19 Controlled 3D orientation of dual-core micromachine.	108
Figure 4-20 Cell culture on magnetic micromachine.	110
Figure 4-21 Multiaxial view (greyscale images) of 3D cell cultures grown on micromachines with purposely-expanded extracellular matrix.	111
Figure 4-22 2D and 3D distributions of cells, respectively.	113
Figure 4-23 Analysing cell distributions under different culture conditions using culture wells.	114
Figure 4-24 Microchip device accommodating swarms of micromachines for conducting dynamic assays.	114
Figure 4-25 DNA hybridisation on a micromachine.	115
Figure 4-26 Result of multiplexed biochemical assays for screening five different target virus DNA strands.	117
Figure 5-1 Magnetic code library.	122
Figure 5-2 Computational simulation of the stray magnetic field of magnetically permeable structures.	123
Figure 5-3 Numerically simulated stray magnetic field patterns (magnetic flux projected on x-y plane) of magnetic microstructures consisting of different core number and core size ratio.	124
Figure 5-4 Build-in capabilities of magnetic codes.	124
Figure 5-5 Schematic illustration of a purpose-built setup of co-axially assembled microcapillaries for synthesis of magnetic codes.	125
Figure 5-6 Fluidic modulation of the emulsion core ratio (top) and the core number (bottom) by regulating the first-step (v_1) and second-step (v_2) emulsification frequencies.	126
Figure 5-7 Micrographs of as-fabricated magnetic microstructures.	127
Figure 5-8 Size distribution and coefficient of variation (CV) of magnetic cores for single-core and dual-core magnetic microparticles.	128
Figure 5-9 Schematic of the electrical measurement setup based on GMR sensor.	129
Figure 5-10 Characteristics of GMR sensor.	129
Figure 5-11 Magnetic flux distribution of a single magnetized sphere.	131
Figure 5-12 External magnetic field for biasing magnetic sensor and magnetising the	

particle to generate the stray magnetic field	132
Figure 5-13 Two approaches for resolving the particle's stray magnetic field using a proximity magnetic sensor	133
Figure 5-14 Motorized scanning system.....	133
Figure 5-15 Normalised sensor voltage profiles obtained by 1D scanning of microstructures of different morphologies.....	134
Figure 5-16 Space ratio changing with size ratio.....	134
Figure 5-17 Schematic showing the reconstruction of 2D stray field information through the raster scanning.....	135
Figure 5-18 Multiple 1D scanned x-axis profiles along the y-axis direction.....	135
Figure 5-19 Reconstructed 2D map of the stray magnetic field distribution.....	136
Figure 5-20 Magneto-fluidic chip	137
Figure 5-21 Fabrication of a magnetofluidic decoder.....	137
Figure 5-22 Time-of-flight detected voltage signals.....	138
Figure 5-23 Radar plot representation of the five different characteristic peak values	139
Figure 5-24 Workflow of a stray magnetic field encoded multiplexed kinetic assay.	140
Figure 5-25 Built-in capability.....	140
Figure 5-26 Fluorescence intensities of the encoded magnetic carriers after incubation with target DNA and fluorescence reporters in the presence (kinetic) and absence (static) of rotational motion.....	141
Figure 5-27 Resolved magnetic field distribution projected on the x-y plane.....	142
Figure 5-28 Results of multiplexing assay.....	142

List of Tables

Table 1-1 Physical restraints on micromachines in different environments	3
Table 1-2 Evaluation of various actuation mechanisms for micromachines.....	11
Table 1-3 Key features of various fabrication methods for microgels.[88]	19
Table 1-4 Biocompatible magmatic material for biomedical and bioengineering applications	24

Abstract

Smart mechanical systems have greatly extended the reach of human beings in sensing, interacting with, and manipulating objects in the microscopic world. In particular, micromachines can expand our capabilities to access small confined and enclosed spaces, and can be employed for monitoring, diagnosis and treatment of diseases. However, developing micromachines for bioanalysis, which requires the smart integration of power sources, multimodal locomotion, dynamic maneuverability and biosensing functions, remain a formidable challenge.

In nature, living organisms including magnetotactic bacteria have leveraged ordered structures to develop smart and adaptive behaviors. Moreover, advanced materials have been endowed with highly anisotropic mechanical strength and extraordinary functions by creating ordered micro- and nanostructures in the material composition. Along these lines, the present PhD dissertation focuses on systematic investigation of smart micromachines with magnetic structural order, which are fabricated by two major approaches, including magnetic field-assisted self-assembly and photolithography, and microfluidics-directed compartmentalisation assembly of magnetic building blocks.

Based on the above approaches, the first investigation focuses on aquatic micromachines with ordered magnetic nanochains. Multiphase and dynamic maneuverability of micromachines are unlocked, which can bypass the physical constraints of diminishing gravity, dominating surface tension and fluidic drag at the microscale. The 2D planar design of micromachine structures, taking advantage of a Euler's disk-inspired magnetic steering mechanism, enables the ultralight aquatic micromachines with high motility and large-area maneuverability.

The next study investigates a microfluidics-directed assembly of magnetic micro-compartments to build micromachines. The approach is shown to tailor the magnetic coupling between the magnetic building blocks, which endows micromachines with 3D-trackable and differentiable motion. Following this study, a unique set of stray magnetic field fingerprints have been revealed by the inter-compartment magnetic coupling. By hierarchically arranging the magnetic compartments using microfluidic emulsion assembly, a library of encoded magnetic micromachines are generated and shown to be readily decodable by a compact giant magnetoresistance sensor, underlying an streamlined kinetic bioassay platform.

In summary, the series of studies presented in this thesis uncover the physics behind a couple of key functionalities, such as multimodal motility, large-area maneuverability, response tunability, and decodability for smart mobile micromachines. The outcomes of this PhD research project, including fundamental robotic control and proof-of-concept demonstration should inspire future development of micromachines for real-world in-vitro and in-vivo bioanalytical applications.